DOI: 10.1143/JPSJ.81.034401

A 461 nm Laser System and Hollow-Cathode Lamp Spectroscopy for Magneto-Optical Trapping of Sr Atoms

Takatoshi AOKI*, Kotaro UMEZAWA, Yuki YAMANAKA, Naotomo TAKEMURA, Yasuhiro SAKEMI[1], and Yoshio TORII

Institute of Physics, Graduate School of Arts and Sciences, University of Tokyo, Meguro, Tokyo 153-8902, Japan
[1]*Cyclotron and Radioisotope Center, Tohoku University, Sendai 980-8578, Japan*

(Received June 29, 2011; accepted December 12, 2011; published online February 8, 2012)

We develop a laser system with a wavelength of 461 nm and a power of 175 mW using a master oscillation power amplifier (MOPA) system and second-harmonic generation (SHG) via a $KNbO_3$ crystal. To stabilize the laser frequency to the atomic absorption line, we measured the saturated absorption spectrum of a Sr hollow-cathode lamp. The dependences of the Lamb dip signal and the frequency modulation spectrum on the pump beam power were observed. The collision broadening due to the Ne buffer gas increased the observed width of the signals in addition to the saturation effect. In spite of such an increased width ($\sim$100 MHz), we demonstrated stable magneto-optical trapping of Sr atoms. The number of atoms obtained, 1×10^7, is sufficient to proceed to various ultracold Sr atoms experiments.

KEYWORDS: laser spectroscopy, laser cooling and trapping, Bose–Einstein condensation, quantum degenerate of mixture, strontium, frequency modulation spectroscopy, hollow-cathode lamp, second harmonic generation, tapered amplifier

1. Introduction

Quantum degenerate gases of atoms have been investigated theoretically and experimentally since they were produced in 1995 owing to the development of techniques of laser cooling and evaporative cooling.[1)] Currently, the interest of physicists shifts to ultracold or quantum degenerate gases of molecules. Compared with atoms, molecules have rich internal states, which include vibrational and rotational states. Moreover, ultracold trapped polar molecules with permanent electric dipole moments have been studied theoretically for new quantum phases[2)] and quantum computations.[3)] Ultracold controlled chemistry is also predicted.[4)] Recently, ultracold polar molecule consisting of two species alkali atoms Rb and K has been realized using a combination of heteronuclear Feshbach resonance and photoassociation via a stimulated Raman adiabatic passage (STIRAP).[5)] The molecule stays in a rovibrational ground state, which has an electric dipole moment of 0.6 D.

In general, alkali-alkali molecules have no electron spin. On the other hand, a molecule consisting of alkali and alkali-earth atoms have an electron spin in the rovibrational ground states. Several theories have predicted new quantum simulators for lattice spin models,[6)] and measurements of fundamental physics[7,8)] using molecules with an electron spin. To produce ultracold molecules comprised of alkali and alkali-earth atoms, we chose a mixture of ultracold Rb and Sr atoms because laser cooling techniques of Rb and Sr atoms are well established. Moreover, the electric dipole moment of the RbSr molecules has been predicted to be 1.36 D,[9)] which is larger than the electric dipole moment of the RbK molecule. The RbSr molecules with the large electric dipole moment can achieve the new quantum phase transitions,[2)] which the RbK molecules can not achieve.

For the laser cooling of Sr atoms,[10)] we need a high power laser whose frequency should be locked to just (or near) the resonance line of Sr atoms. It is necessary to warm the Sr oven to a temperature of 400 °C to achieve sufficient pressure for Sr spectroscopy. However, at this temperature, the window of the oven is easily contaminated by the chemical reaction between the oven window and the Sr atomic vapor. In contrast, the Sr hollow-cathode lamps, where Sr vapor is produced by sputtering from a hollow-cathode intrasurface by electrostatic discharge, are operated at room temperature. In spite of its convenience, spectroscopy using a Sr hollow-cathode lamp has not yet been reported in the literature.

In this paper, we report a laser system with a wavelength of 461 nm, and the spectroscopy of a Sr hollow-cathode lamp. In addition, we demonstrate an experiment on the magneto-optical trapping of Sr atoms. First, we show the laser system and experimental setup for hollow-cathode lamp spectroscopy. Next, we discuss the experimental results of Doppler free spectroscopy and frequency modulation. Finally, we describe the results of the demonstration of the laser cooling and magneto-optical trapping of Sr atoms.

2. Experimental Apparatus

The wavelength for the laser cooling of Sr atoms via the transition between $^1S_0$ and $^1P_1$ is 461 nm. We fabricated a master oscillation power amplifier (MOPA) system with a wavelength of 922 nm, and a system for second-harmonic generation (SHG) of 461 nm. Figure 1 shows the laser system of MOPA and SHG. The laser beam injected from the external cavity diode laser (ECDL) in Littrow configuration with a wavelength of 922 nm is amplified through a tapered amplifier (TA). The diode laser (DL) chip in ECDL is antireflection-coated (Eagleyard EYP-RWE-0940-08000-0750-SOT01-0000). The TA chip is also antireflection-coated (Eagleyard EYP-TPA-0915-01500-3006-CMT03-0000). Aspheric lenses with a focal length of 4.5 mm and NA = 0.55 (Thorlabs C230TM-B) are used for collimating

*E-mail: aoki@phys.c.u-tokyo.ac.jp

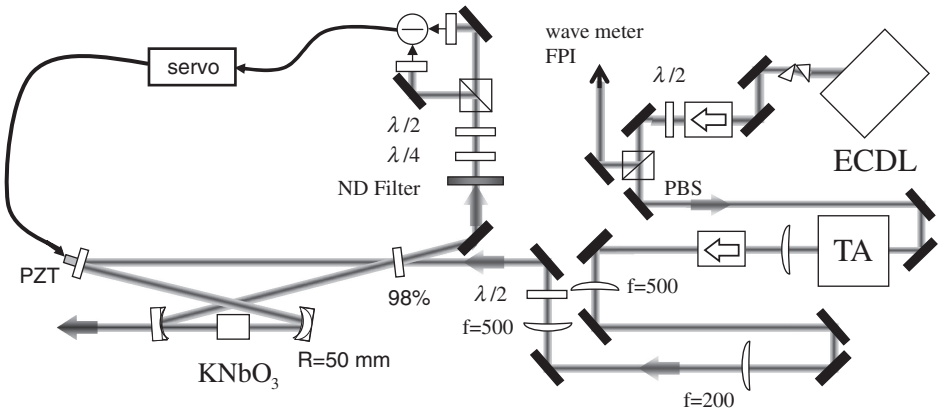

Fig. 1. 461 nm laser sysyem. A laser beam from a 922 nm ECDL, after being amplified by a TA, enters the SHG cavity to generate a 461 nm laser beam.

the laser beam from DL and for focusing the laser beam from ECDL onto the TA chip. The amplified TA beam is collimated by another aspheric lens with a focal length of 2.75 mm and NA = 0.65 (Thorlabs C390TM-B), and a cylindrical lens with a focal length of 50 mm (Thorlabs LJ1695RM-B). These aspheric lenses are located inside the ECDL and TA boxes (not shown in Fig. 1).

Figure 2(a) shows the output power of TA. The injected power was 27 mW. With increasing TA current, the output power increased. An output power of 900 mW after the optical isolator (60 dB) was obtained at a TA current of 2.45 A. Then, the amplified laser beam was mode-matched to the SHG cavity. The SHG cavity consists of four mirrors and a $KNbO_3$ crystal. The reflectivity of the mirror M1, R_1, is 98%, while those of other mirrors, R_2, R_3, and R_4, are more than 99.5%. The curvatures of the concave mirrors M3 and M4 are 50 mm. The transmittance of M3 and M4 for 461 nm beams is 90%. The mirror M2 is attached to a PZT to tune the cavity length. The distance between M3 and M4 is 59 mm. The beam waist at the center of the crystal is 46 μm. The crystal is $3 \times 2.8 \times 5\,\text{mm}^3$. From the observed transmittance signal through the SHG cavity, the FWHM of the SHG cavity was 5.9 MHz, the FSR was 0.79 GHz, the finesse was 133, and the enhancement factor of intracavity power was estimated to be 37.

For the cavity resonance frequency to be tuned to the ECDL frequency, we used the Hänsch–Couillaud technique.[11] The differential error signal obtained was used to stabilize the cavity length to keep the maximum intracavity power. The piezo actuator used to tune the cavity length has a resonance frequency of 138 kHz. The crystal cut at 42° off with respect to the *b*-axis in the *ab*-plane of the crystal is phase-matched at a temperature of 23° to obtain a 461 nm power. Figure 2(b) shows the 461 nm power generated via the SHG cavity measured by changing the input (922 nm) power. The solid curve is a theoretical fit using the square of the input power. Optimizing the temperature of the $KNbO_3$ crystal results in a 461 nm power of 175 mW. The fluctuation in intensity was about 5%. At higher input powers (>500 mW), the obtained SHG power dependence is in good agreement with the theoretical power dependence. At lower input powers, the obtained output power is lower than the theoretical value. This is because we aligned the SHG cavity and optimized the temperature of the crystal only for higher powers. If we optimize the system for lower powers, it is expected that SHG power will fit the theoretical curve for the entire range of input powers.

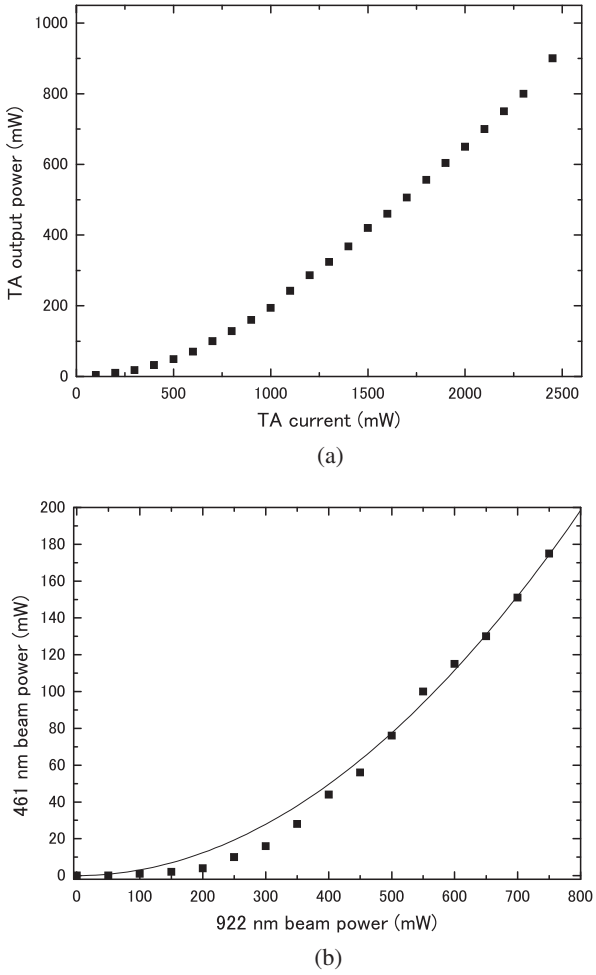

Fig. 2. (a) TA output power vs TA current, (b) generated 461 nm power vs incident 922 nm power. The solid line is a theoretical curve fitting to the SHG power.

The spectroscopy apparatus is shown in Fig. 3. The laser beam from the SHG cavity is split by a polarizing beam splitter (PBS). Then, one of the resulting beams is divided into a probe beam and a pump beam by another PBS. For frequency modulation spectroscopy,[12,13] the probe beam

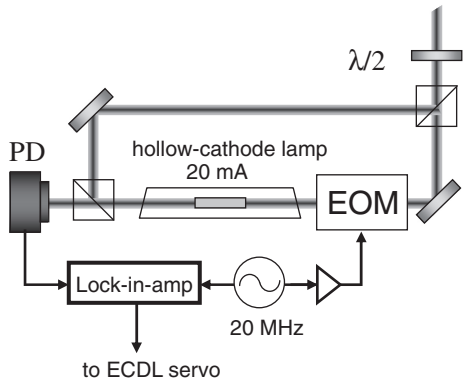

Fig. 3. Schematic diagram of hollow-cathode lamp spectroscopy. The 461 nm laser beam was divided into a pump beam and a probe beam. The probe beam goes through the electro-optic modulator with a frequency of 20 MHz.

goes through an electro-optic modulator (EOM) before entering a Sr hollow-cathode lamp (Hamamatsu Photonics L2783-38NE-SR). The pump beam is counterpropagating through the lamp. The power of the probe beam is detected by a fast photo-detector (PD). The electric signal from the PD goes to a fast lock-in amplifier (Stanford Research SR844, with a bandwidth with a maximum frequency is 200 MHz). A modulation signal with a frequency $\omega_{\mathrm{mod}} = 20$ MHz from a function generator is fed to the EOM (after amplified to 1 W) and the reference input of the lock-in amplifier. The output signal from the lock-in amplifier is monitored by an oscilloscope and fed to a servo circuit to control the PZT on the grating in the ECDL for frequency stabilization.

3. Results and Discussion

3.1 Hollow-cathode lamp spectroscopy

First, we measured the Doppler free saturation spectrum by monitoring signals from the PD by an oscilloscope (EOM was kept off). The ECDL frequency was scanned by sweeping the voltage of the grating PZT around a wavelength of 921.623 nm. The frequency of the SHG beam is twice this DL frequency. Figure 4(a) shows the typical transmission signal of the probe beam as a function of the SHG frequency. The frequency of the 461 nm laser beam was swept with a frequency of 1 Hz and a width of 5.67 GHz, which is calibrated by monitoring the transmission of a Fabry–Pérot cavity. The absorption signal had a Lamb dip at the center of a Doppler-broadened absorption profile. The powers of the probe beam and pump beam were 0.05 and 3 mW, respectively. The full width at half maximum (FWHM) of the dip was 126 MHz. The saturation intensity I_{s} of the Sr 461 nm line is 42 mW/cm^2. A pump beam power of 0.07 mW corresponds to $I/I_{\mathrm{s}} = 1$.

Figure 4(b) shows the error signal obtained by using frequency modulation spectroscopy. The time constant and sensitivity of the lock-in-amplifier were 10 ms and 30 μV, respectively. By sweeping the frequency of ECDL, the derivative of the absorption curve shown in Fig. 4(a) was obtained. The large derivative curve is due to the Doppler-broadened absorption profile. The sharp derivative curve at the center is due to the Lamb dip. The width of peak-to-peak voltage for this sharp signal was 114 MHz.

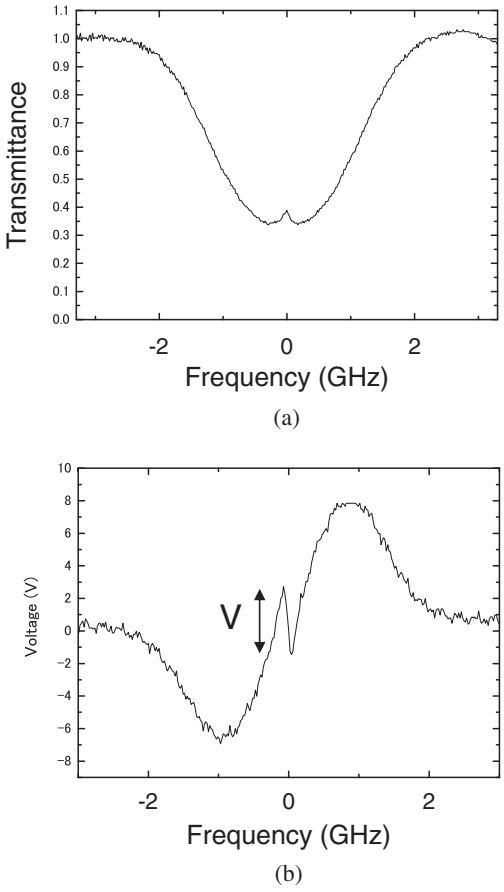

Fig. 4. Signals of hollow-cathode lamp spectroscopy. (a) Doppler-free saturation absorption signal. The Lamb dip signal is observed at the bottom of a broad Doppler absorption profile. (b) A frequency modulation signal has a differential profile of (a). The differential shape obtained at the center is the error signal to utilize frequency stabilization.

To stabilize the laser frequency, it is important to obtain a larger gradient of the error signal slope. Hence, a larger peak-to-peak voltage and a narrow width are preferable. For this reason, we measured the dependence of the signal width on the pump beam power, as shown in Fig. 5(a). The open circles are the widths Γ of the Lorentzian function fit to the Lamb dip signals, and the filled circles are the peak-to-peak widths of the FM signals. The solid curve is the theoretical width fit to the experimental data taking into account the combination of the saturation effect and the pressure broadening $\Gamma = \gamma_{\mathrm{n}}\sqrt{S_0 + (1 + \gamma_{\mathrm{p}}/\gamma_{\mathrm{n}})^2}$,[14] where Γ is the width of the Lorentzian function fit to the Lamb dip, γ_{n} the natural width 34 MHz for the $^1S_0$ to the $^1P_1$ line in the Sr atom, $S_0 = I/I_{\mathrm{s}}$ the saturation parameter, and γ_{p} the pressure broadening due to the Ne buffer gas. To our knowledge, there are no available value of γ_{p} of Sr and Ne in the literature. Thus, we determined it experimentally. Fitting to the observed width results in $\gamma_{\mathrm{p}} = 25$ MHz. The pressure of the Ne buffer gas is 5 Torr for our Sr hollow-cathode tube, so it gives 5 MHz/Torr. This value was obtained only with a constant pressure. In frequency modulation spectroscopy, the modulation index M was 1.4. Because of $M\omega_{\mathrm{mod}} < \Gamma$, the theoretical width between peak-to-peak FM signals is given by differentiating Lorentzian function with respect to frequency, which is $\Gamma/\sqrt{3}$.[15] The values of the dashed curve

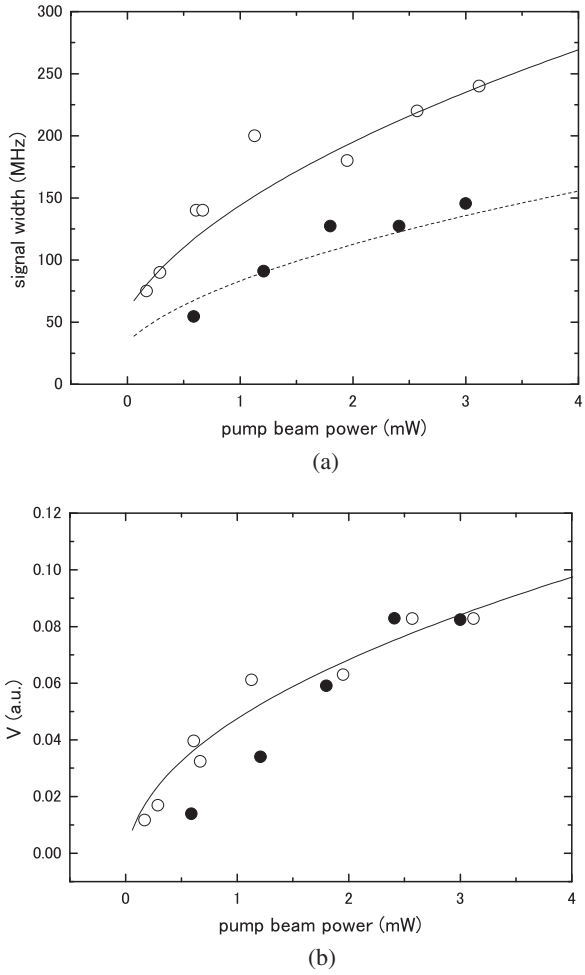

Fig. 5. (a) Width Γ of Lorentzian function fitting to Lamb dip (open circles), and width between peak-to-peak FM signals (filled circles). Theoretical curve fitting to Lamb dip (solid line) and FM signal (dashed line). (b) Height of Lamb dip (open circles) and peak-to-peak FM signal (filled circles). The solid line is a theoretical curve fitting to the Lamb dip and FM signal.

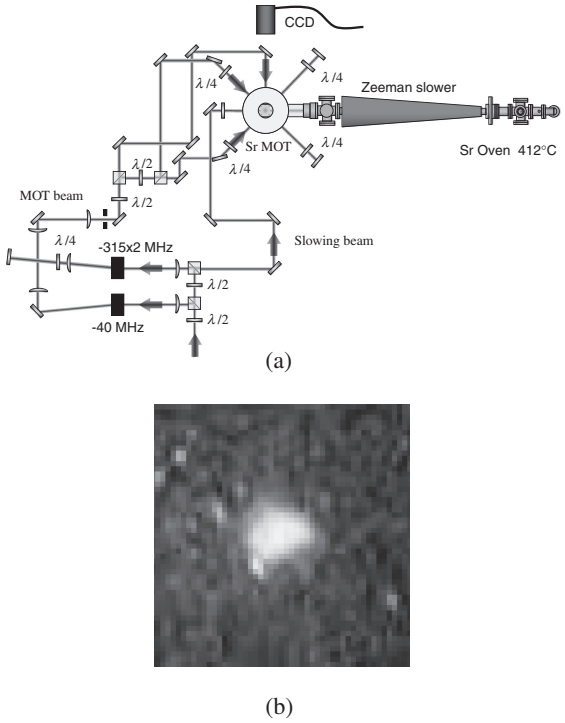

Fig. 6. (a) Optical setup of magneto-optical trap of Sr atoms. The black boxes are acousto-optic modulators (AOMs). (b) Fluorescence image of magneto-optical trap of Sr atoms. The image was monitored on a charge-coupled device camera. The field of view for the image is $4.7 \times 4.5\,\mathrm{mm}^2$.

in Fig. 5(a) is the value of the solid curve divided by $\sqrt{3}$. The widths of FM signals almost fit to this function.

Then, we measured the dependence of the heights of the signals on the pump beam power, as shown in Fig. 5(b). The open circles are the heights of the Lamb dip signals. The filled circles are the peak-to-peak voltages obtained by FM spectroscopy. Both data are normalized so that the heights of the Lamb dip and FM signals overlap. The solid curve is a fit to the experimental data using the function $S_0/\sqrt{1+S_0}$.[16] The obtained signals of the Lamb dip and the FM signals are in good agreement with the theoretical prediction.

After the above measurement, we stabilized the laser frequency using the FM signal. Taking into account the above results, higher pump power offers a larger gradient of the FM signal, and is preferable for the frequency stabilization. But we also need the laser power of trapping beams. So we chose 3 mW as the pump power. The frequency fluctuation was supressed to about 1 MHz, estimated by residual fluctuation, which is 1/100 of the peak-to-peak FM signal. This fluctuation is much smaller than the natural line width of 34 MHz. Thus, it does not affect the fluctuation in the number of trapped atoms or temperature in the trapping experiment.

The Sr atom has several isotopes, i.e., ^{88}Sr, ^{87}Sr, ^{86}Sr, and ^{84}Sr. The natural abundances of these species are 82.58, 7.00, 9.86, and 0.56%, respectively. The isotope shift of ^{86}Sr and ^{84}Sr relative to ^{88}Sr are -125 and -271 MHz.[17] Fermionic ^{87}Sr has a hyperfine structure of $F = 7/2$, $11/2$, and $9/2$ in the excited state $^1P_1$, whose energies are -12, -55, and -78 MHz, respectively, shifted from the ^{88}Sr transition,[18] where F is the total angular momentum of the electric angular momentum and nuclear spin. We can not observe any signal there other than that of ^{88}Sr because of the low natural abundance. The ^{87}Sr signals are almost involved in the ^{88}Sr broad Lamb dip signal of about 200 MHz, where the height of the expected isotope signal is comparable to the magnitude of noise.

3.2 *Magneto-optical trapping of Sr atoms*

We constructed an optical system for the laser cooling of Sr atoms, as shown in Fig. 6(a). The laser beams from the SHG cavity is split by a PBS. One beam is used for the spectroscopy of the Sr hollow-cathode lamp, as mentioned above. The other beam is further split by a PBS into two beams: MOT beam and slowing beam. Each beam goes through an acousto-optic modulator (AOM) to tune its frequency. The detunings of these beams are -40 and -640 MHz, respectively. The large detuning of the slowing beam is realized by a double-pass AOM. The experimental procedure is as follows. First, the Sr atomic beam outgoing from an oven at a temperature of 673 K was decelerated by a counterpropagating circularly polarized slowing beam in the region of the increasing-type Zeeman slower. The slowing

beam power was 8 mW. Then, slowed atoms were loaded into a magneto-optical trap (MOT) using six orthogonal circularly polarized MOT beams. The powers of four MOT beams propagating in the horizontal plane were 8 mW, while the powers of two beams propagating in the vertical direction were 4 mW. The magnetic gradient was 160 G/cm generated by water-cooled anti-Helmholtz coils at a current of 50 A. We optimize the slower magnetic field by changing the current through the Zeeman profile and as well as the bias coils by monitoring the fluorescence from the trapped atoms. The magnetic fields at the entrance and exit of the Zeeman slower are about 120 and 420 G, respectively.

The fluorescence signal from the trapped atoms was collected by a lens and was imaged onto a charge-couple-device (CCD) camera. Figure 6(b) shows the obtained image of the cloud of trapped atoms. From the image, we estimated the number of trapped atoms. By comparing the fluorescence signal from the MOT with the power of the reference beam incident to the CCD camera, the power of fluorescence was estimated to be 120 nW. Taking into account the solid angle of the lens attached to the camera and the spontaneous-emission rate from the trapped atoms, the number of atoms was evaluated to be 1×10^7.

4. Conclusions

We developed a 461 nm laser system and a hollow-cathode lamp spectroscopy system for the laser cooling of Sr atoms. The MOPA system consisting of ECDL and TA produced a 922 nm laser beam with a high power of up to 900 mW. The SHG cavity using the $KNbO_3$ crystal generated a high-power cw 461 nm laser beam up to 175 mW.

We performed hollow-cathode lamp spectroscopy for laser stabilization to the Sr absorption line. The obtained width and height of the Lamb dip and FM signal were in good agreement with theoretical predictions. The pressure-broadened width of Sr atoms due to the use of a 5 Torr Ne buffer gas was determined to be 25 MHz. Finally, we demonstrated the magneto-optical trapping of Sr atoms. The number of trapped atoms was 1×10^7. This atom number is sufficient for making BECs of Sr, which has recently been reported.[19)]

Currently, we are preparing simultaneous MOT of Rb and Sr atoms. The differences in oven temperatures and the properties of the required Zeeman slower for Rb and Sr have made it difficult to realize the simultaneous laser cooling and trapping. We believe that this mixture of alkali and alkaline-earth atoms will present a system for investigating the new quantum phases and a diagnostic tool in this field.

Acknowledgments

We thank Dr. A. Yamaguchi (PTB) and Dr. S. Uetake (Kyoto University) for discussions of MOPA and SHG systems. This research is supported by the Matsuo Foundation, and a Grant-in-Aid for Scientific Research on Innovative Areas "Extreme quantum world opened by atoms" (No. 21104005) from the Ministry of Education, Culture, Sports, Science and Technology, Japan.

1) E. A. Cornel and C. E. Wieman: Rev. Mod. Phys. **74** (2002) 875; W. Ketterle: Rev. Mod. Phys. **74** (2002) 1131.
2) H. P. Büchler, E. Demler, M. Lukin, A. Micheli, N. Prokof'ev, G. Pupillo, and P. Zoller: Phys. Rev. Lett. **98** (2007) 060404.
3) D. DeMille: Phys. Rev. Lett. **88** (2002) 067901.
4) L. D. Carr, D. DeMille, R. V. Krems, and J. Ye: New J. Phys. **11** (2009) 055049.
5) K.-K. Ni, S. Ospelkaus, M. H. G. de Miranda, A. Peér, B. Neyenhuis, J. J. Zirbel, S. Kotochigova, P. S. Julienne, D. S. Jin, and J. Ye: Science **322** (2008) 231.
6) A. Micheli, G. K. Brennen, and P. Zoller: Nature **2** (2006) 341.
7) E. R. Meyer and J. L. Bohn: Phys. Rev. A **80** (2009) 042508.
8) T. Aoki, K. Umezawa, Y. Torii, and Y. Sakemi: Proc. Fundamental Physics using Atoms, 2010, p. 101.
9) P. S. Zuchowski, J. Aldegunde, and J. M. Hutson: Phys. Rev. Lett. **105** (2010) 153201.
10) T. Kurosu and F. Shimizu: Jpn. J. Appl. Phys. **29** (1990) L2127.
11) T. W. Hänsch and B. Couillaud: Opt. Commun. **35** (1980) 441.
12) J. L. Hall, L. Hollberg, T. Baer, and H. G. Robinson: Appl. Phys. Lett. **39** (1981) 680.
13) S. Watanabe, Y. Aizawa, and A. Morinaga: Jpn. J. Appl. Phys. **42** (2003) 1462.
14) U. Dammalapati, I. Norris, and E. Riis: J. Phys. B **42** (2009) 165001.
15) J. M. Supplee, E. A. Whittaker, and W. Lenth: Appl. Opt. **33** (1994) 6294.
16) W. Demtröder: *Laser Spectroscopy* (Springer, Heidelberg, 2008) 4th ed.
17) M. Anselment, S. Chongkum, K. Bekk, S. Göring, A. Hanser, G. Meisel, and H. Rebel: Z. Phys. D **3** (1986) 421.
18) A. D. Ludlow: Ph. D. thesis, Faculty of the Graduate School, University of Colorado, United States (2008).
19) P. G. Mickelson, Y. N. Martinez de Escobar, M. Yan, B. J. DeSalvo, and T. C. Killian: Phys. Rev. A **81** (2010) 051601(R).